Environmental Science Processes & Impacts

ROYAL SOCIETY OF CHEMISTRY

PAPER

View Article Online
View Journal

Cite this: DOI: 10.1039/d5em00943j

Atmospheric fate of 4:2 fluorotelomer alcohol using an oxidation flow reactor and proton transfer reaction time-of-flight mass spectrometry

Alessia A. Colussi, [a] Trevor C. VandenBoer, [a] Cora J. Young *[a] and John Liggio*[b]

Commonly used methodologies applied to studying the atmospheric degradation of per- and polyfluoroalkyl substances (PFAS) require analyses to be conducted offline and under dry conditions, potentially limiting the atmospheric relevance of the resulting mechanism and kinetics. We coupled an oxidation flow reactor (OFR) to a proton transfer reaction time-of-flight mass spectrometer (PTR-ToF-MS), focusing on the NO_x-free oxidation of a perfluorocarboxylic acid precursor – the 4:2 fluorotelomer alcohol (FTOH) – in the first application of this system to PFAS. The PTR-ToF-MS was calibrated under dry conditions (0 to 1% RH) and at relative humidities (RHs) of 22%, 44%, and 60%. The oxidation of 42 FTOH by $^{\bullet}OH$ radicals was observed in real-time, as a function of RH, with PTR-ToF-MS detecting both primary and secondary 4:2 FTOH degradation products: the 4:2 fluorotelomer aldehyde and 4:2 fluorotelomer carboxylic acid, respectively. The resulting pseudo-first-order kinetics (k_{obs}) were determined and compared to previously reported FTOH values. The determined k_{obs} values were $(1.0 \pm 0.1) \times 10^{-12}$ (22% RH), $(7.4 \pm 0.8) \times 10^{-13}$ (44% RH), and $(7.2 \pm 0.8) \times 10^{-13}$ cm^3 $molecules^{-1}$ s^{-1} (60% RH), comparable to prior reports at 22% RH and lower as RH increased. This type of experiment demonstrates that the OFR-PTR-ToF-MS technique can be transferred to study other suspected, but uncharacterized, atmospheric PFAS transformations.

Received 14th November 2025
Accepted 3rd February 2026

DOI: 10.1039/d5em00943j

rsc.li/espi

Environmental significance

Volatile per- and polyfluoroalkyl substances (PFAS), such as fluorotelomer alcohols (FTOHs), can be emitted into the atmosphere from industrial and commercial sources. Their degradation leads to the formation of persistent perfluorocarboxylic acids, detected globally in urban, rural, and 5 remote regions. Previous studies on FTOH oxidation were conducted under dry conditions, 6 limiting their atmospheric relevance. Here, we investigate the OH oxidation of 4:2 FTOH under 7 NO_x-free and humid conditions using an oxidation flow reactor coupled to proton transfer reaction time-of-flight mass spectrometry. We observed decreasing reaction rates with increasing humidity, highlighting the need to consider water vapour in FTOH chamber experiments and models. This work provides more representative kinetics for atmospheric models, supporting improved 11 understanding of PFAS transport and environmental fate.

1 Introduction

For over seven decades, a diverse group of synthetic, fluorinated organic compounds known as per- and polyfluoroalkyl substances (PFAS) have been widely used for industrial and commercial applications. Due to the strength and stability of the carbon–fluorine bond, PFAS have ideal chemical properties, such as hydrophobicity and lipophobicity, and are utilized in various applications (*e.g.*, food packaging, textiles, electroplating of metals).[1] They can enter the atmosphere directly *via* emissions from manufacturing facilities, wastewater treatment plants, landfills, *etc.*,[1,2] and their terminal acid degradation products are very resistant to metabolic and environmental degradation.[3] Additionally, some PFAS are considered toxic and bioaccumulative; high levels of PFAS exposure have been associated with adverse health effects in humans[4–7] and wildlife.[8–12]

Volatile and semi-volatile atmospheric PFAS, such as fluorotelomer alcohols (FTOHs), are used in the fluoropolymer and surfactant industry and as chlorofluorocarbon replacements.[13] They are included in the formulations of a variety of products such as adhesives, polishes, paints, and electronic materials[14] and in some cases, the FTOHs can be released directly into the environment from product use.[15] In 2006, the global production of FTOHs was estimated to be between 11 to 14×10^6 kg $year^{-1}$ with 40% of that production occurring in North America.[16,17] This group of compounds has an estimated atmospheric half-life of 10 to 20 days and are able to be

[a]Department of Chemistry, York University, Toronto, ON, Canada. E-mail: youngcj@yorku.ca

[b]Air Quality Research Division, Environment and Climate Change Canada, Toronto, ON, Canada. E-mail: john.liggio@ec.gc.ca

widespread to achieve relatively uniform hemispheric distribution.[18] Several studies have reported gas-phase FTOHs at tens to hundreds of pg m^{-3} in samples from around the world.[19–22] Thus, their atmospheric degradation has been deemed as a plausible contributing source of perfluorocarboxylic acids (PFCAs) found in remote locations such as the Arctic.[23,24]

The atmospheric fate of gas-phase FTOHs has been the subject of several prior investigations, all of which used smog chambers and Fourier transform infrared spectroscopy (FTIR).[16,18,19] More recently, a chamber coupled with mass spectrometry enabled continuous measurements of the degradation products of hydrofluoroether alcohols, a subclass of PFAS, for the first time.[25] Collectively, these smog chamber studies—including the recent work on hydrofluoroether alcohols—were conducted under dry conditions, in part to minimize interference from water vapour. Water is a well-known interferent in smog chamber studies employing methods such as fluorine-19 nuclear magnetic resonance spectroscopy (^{19}F NMR),[26] FTIR,[27] and modern mass spectrometry techniques like iodide adduct chemical ionization mass spectrometry (I-CIMS).[28–32] As a result, although the effects of water vapour on the oxidation kinetics of non-fluorinated alcohols (20% to 95% relative humidity, RH)[33–38] have been explored to some extent, comparable data for fluorinated analogues such as FTOHs are lacking. Here we revisit the degradation of 4:2 FTOH under dry and humidified conditions to expand our mechanistic understanding of the atmospheric chemistry of this compound.

In this work, we apply a proton transfer reaction time-of-flight mass spectrometer (PTR-ToF-MS) to the study of 4:2 FTOH oxidation by coupling it to an oxidation flow reactor (OFR). This new approach to measuring gas-phase PFAS allows us to examine its atmospheric degradation and formation of products, both facilitated by $^{\bullet}$OH radicals. The use of OFR-PTR-ToF-MS can overcome the experimental limitations of performing oxidation chemistry under more atmospherically relevant RH conditions in the absence of NO_x ($NO + NO_2$). This work shows that: (i) a PTR-ToF-MS can be used to measure gas-phase PFAS, (ii) 4:2 FTOH degradation products can be identified in real-time using PTR-ToF-MS, and (iii) OFR experiments can be used to study the degradation kinetics of 4:2 FTOH and, by extension, many other volatile PFAS.

2 Materials and methods

2.1 OFR experiments

A custom-built OFR was used in these chamber experiments (Fig. S1) which has been described and characterized previously.[39–41] The current reactor is a fused quartz flow tube with a cone-shaped diffusion inlet and seven outlets. Six of the outlets act as exhaust to reduce gas-phase wall losses and to maintain plug flow.[39] The flow rate through the 16 L OFR was approximately 2 L min^{-1}, resulting in a residence time of 8 min. Using the density of air (1.293 kg m^{-3}) and dynamic viscosity of air (1.714×10^{-5} Pa s),[42] a Reynolds number of 16 was calculated to confirm laminar flow within the OFR during all experiments. These reactors utilize oxidants at concentrations considerably higher than the ambient atmosphere to accelerate oxidation chemistry.[43] Within minutes, exposures equivalent to multiple days or weeks of atmospheric oxidation are possible. These higher-than-ambient concentrations are generated by the photolysis of a chosen oxidant precursor using low-pressure ultraviolet (UV) lamps. Compared to traditional smog chambers, the rapid oxidation timeframes result in shorter sample residence times and reduced wall effects within an experiment.[44,45]

Oxidation flow reactors have been used to infer the transition between functionalization (*i.e.*, oxygen addition)[46] and fragmentation (*i.e.*, carbon–carbon bond cleavage)[47] for volatile organic compounds (VOCs), and the subsequent impact of these processes on secondary organic aerosol formation.[40,46,48] It has been noted that these experimental conditions may not fully reflect ambient reaction pathways under all conditions and thus OFRs may have limits on their atmospheric relevance, particularly associated with oxidant formation and alkylperoxy radical (RO_2) chemistry.[43,49,50] The low-NO_x experiments described in this work follow the standard methodology consistent with OFR best practices; however, one limitation specific to this work is the elevated concentrations of $^{\bullet}HO_2$ radicals within the reactor relative to typical atmospheric levels. This increased HO_2 abundance can alter the radical chemistry by favouring RO_2 + HO_2 reactions over RO_2 + NO pathways, which can lead to differences in product distributions. Nonetheless, given that this study does not aim to quantitatively resolve product distributions, the influence of altered radical pathways is not expected to affect the main findings.

Approximately 750 parts-per-billion-by-volume (10^{-9} mol mol^{-1}, ppbv) of externally generated ozone (O_3, model TG-10; Ozone Solutions, San Antonio, TX, USA) was introduced into the OFR and was photolyzed using UV light at 254 nm provided by low-pressure mercury lamps (part # 82-3309-9; Jelight Company Inc., Irvine, CA, USA). This produces O (^{1}D), which reacts with water vapour to generate OH. This method is a well-established approach in OFR studies[43,51–54] and produces a steady-state OH concentration that can be quantitatively estimated using a CO tracer. Radical production is influenced by O_3 and H_2O concentrations as well as UV lamp intensity, and this configuration is relatively resilient to OH suppression at O_3 levels reaching up to 70 parts-per-million (ppm) due to a higher OH concentration and enhanced HO_2 recycling, which helps maintain stable radical chemistry.[53] In the absence of light, we performed negative control experiments of 4:2 FTOH in the presence of residual O_3 to measure whether any loss took place on the timescales present in this system. The average temperature inside the OFR was 23.0 ± 0.7 °C and the RHs were controlled at 21.8 ± 0.7%, 44.0 ± 3.9%, and 59.6 ± 5.5% (model HMP60; Vaisala Oyj, Vantaa, Finland). The OH levels within the OFR were adjusted using the voltages applied to, and the number of, UV lamps. The OH exposure—the product of the average residence time in the reactor and OH concentration—was then estimated by measuring the rate of decay of carbon monoxide (CO)[55] during offline calibrations (Fig. S2). Both CO and O_3 were measured using standard gas analyzers (CO by model 23r; ABB Inc—Los Gatos Research, San Jose, CA, USA, and O_3 by model 202; 2B Technologies, Broomfield, CO, USA).

The OH exposure values were determined using the second-order rate constant between CO and OH ($(1.54 \pm 0.14) \times 10^{-13}$ cm^3 molecules^{-1} s^{-1})[56] and the resulting photochemical ages were calculated assuming a global average OH concentration (1.50×10^6 molecules cm^{-3})[57] (Section S1). The calculated OH exposure ranged from 1.94×10^{11} to 2.68×10^{12} molecules s cm^{-3}, and the corresponding photochemical ages at each RH are provided in Table S1.

2.2 PTR-ToF-MS measurements

A PTR-ToF-MS (Ionicon Analytik GmbH, Innsbruck, Austria) acquiring data at 0.5 Hz was used to measure the 42 FTOH as it reacted with $^{\bullet}$OH radicals in real-time. The PTR-ToF-MS operating principles and its applications have been described in detail elsewhere.[58–62] Here, the PTR-ToF-MS drift tube pressure was maintained at 2.15 mbar and the electric field at a 600 V difference. The resulting electric field strength (E) and buffer gas density (N) ratio was 140 Townsend. The mass-to-charge ratio (m/z) of the ions are determined by the measured flight times, and an entire mass spectrum ($m/z \leq 480$) is produced with every pulse. Trichlorobenzene (housed in a permeation tube) was continuously added to the inlet to monitor m/z calibration of the instrument. The raw mass spectra were acquired using TofDaq (Tofwerk AG, Thun, Switzerland) and analyzed using Tofware (Tofwerk AG, Thun, Switzerland). The instrument resolution was approximately 3500 $m/\Delta m$ for the 42 FTOH (exact m/z 265.027492) and high-resolution fitting provided analyte signal intensity based on their exact mass with 15 ± 1 ppm accuracy. Due to RH-dependent m/z shifts, observed masses for the reagent ion as well as 4:2 FTOH and its degradation products varied slightly across experiments. However, all values remained within the instrument's mass accuracy specification of 15 ± 1 ppm. Therefore, the exact protonated masses were used throughout for analyte identification and reporting.

Calibration was performed by delivering gas-phase 4:2 FTOH (2101-3-95; SynQuest Labs, Alachua, FL, USA) to the PTR-ToF-MS using a custom-made, temperature-controlled permeation device (PD).[63] Approximately 250 μL of 4:2 FTOH was added to a 60 mm perfluoroalkoxy tube (3.2 mm inner diameter with 5 mm outer diameter, part # 5733K73; McMaster-Carr, Aurora, OH, USA) and thermally sealed on both ends, allowing for a consistent mass of 4:2 FTOH gas to permeate at a constant temperature and pressure.[63,64] The PD was housed in an aluminum block that was temperature controlled using a cartridge heater and was regulated to 75.0 ± 0.1 °C, while 10 mL min^{-1} of dry nitrogen gas flowed over the PD. The mass emission rate was quantified gravimetrically over 26 weeks as 254 ± 2 ng min^{-1} (Fig. S3). Calibrations covered 3 to 21 ppbv of 42 FTOH and were performed under RH conditions relevant to each experiment, which spanned 22%, 44%, and 60% RH (Section S2 and Fig. S4) using m/z 265.02749. This was required due to the potential for water vapour altering the instrument response. Calibrations were done through the OFR in the absence of light and O_3, with mixing ratios controlled by increasing the dilution flow. Zero air passed through a heated platinum catalyst held at 350 °C was used to acquire a background signal which was then subtracted from each calibration point and normalized to the isotope of the hydronium reagent ion ($H_3{}^{18}O^+$, m/z 21.022635) to generate instrument measurements with units of normalized counts per second (ncps).

2.3 Data treatment: rate constant, k_{obs}

The rate constant (k_{obs}, cm^3 molecule^{-1} s^{-1}) for $^{\bullet}$OH radicals with 4:2 FTOH was determined by measuring the decrease in FTOH signal as a function of OH exposure (Section S3). Wall loss due to diffusion to the OFR surfaces can lead to lost analyte signal. Using the diffusion coefficient of 1-hexanol as a proxy,[65] the estimated diffusion time across the reactor radius for 42 FTOH molecules was 417 s, slightly shorter than the experimental OFR gas residence time of 468 s. Given the similarity between these two values, the impact of surface effects was examined by fitting the system response times to single and double exponential functions during the calibration (Table S2) and k_{obs} determinations (Table S3) at each RH (see Section 3.2).

3 Results and discussion

3.1 PTR-ToF-MS: technique for measuring gas-phase PFAS

There are few reports considering the applicability or limitations of using atmospheric mass spectrometry techniques for the detection of volatile PFAS in ambient air compared to controlled lab conditions. Here, the sensitivity and two-second limit of detection (LOD, assuming a signal-to-noise ratio of 3) for 4:2 FTOH under dry conditions were $(12.7 \pm 0.6) \times 10^{-3}$ ncps ppbv^{-1} and 63 parts-per-trillion by volume (10^{-12} mol mol^{-1}, pptv), respectively (Section S4 and Table S4). The average sensitivity ($(70.4 \pm 2.3) \times 10^{-4}$ ncps ppbv^{-1}) and LOD (109 pptv) under humidified conditions was used for the corresponding experiments. Gaseous 42 FTOH has not been previously measured using PTR-ToF-MS and so the sensitivity and LOD values reported here cannot be directly compared to other studies. Rather, we directly compare against that of other common VOCs measured *via* PTR-ToF-MS. The sensitivity value reported here is much smaller than the sensitivity for common VOCs like acetone (30.9 ncps ppbv^{-1})[66] and ethanol (99.23 ncps ppbv^{-1}).[67] The lower sensitivity here is reasonable as we would expect FTOHs to have lower proton affinity (PA) than other VOCs due to the electron-withdrawing properties from fluorination. While the PA for 4:2 FTOH has not been reported, that of 1:2 FTOH is 700 kJ mol^{-1}.[68] The length of the perfluorinated chain has little effect on FTOH properties;[13] hence, it is reasonable to assume the PA of the 4:2 FTOH is ~700 kJ mol^{-1}. This PA is similar to that of water (691 kJ mol^{-1})[69] but lower than those of commonly measured VOCs, such as n-propanol (786 to 791 kJ mol^{-1})[70] and acetone (812 kJ mol^{-1}).[71] Our 42 FTOH LOD was also found to be in a comparable range to that reported for acetone using PTR-ToF-MS[72–74] (Table S5), but higher than 4:2 FTOH measured by I-CIMS (7.9 pptv[75] and 2.9 pptv[76]). We note these LODs are orders of magnitude too high to detect ambient FTOHs because average measurements in North America (Table S6), Europe, and Asia have not exceeded 220 ng m^{-3} (0.022

pptv).[1,16,22,77–79] The Vocus—a PTR-ToF-MS with the highest sensitivity and resolving power on the market—has reported LODs for common VOCs from 10 to 90 pptv[72–74] (Table S5), which suggests even it would be unable to detect ambient FTOHs. Thus, a Vocus, a traditional PTR-ToF-MS, and an I-CIMS are not sufficiently sensitive for the detection of ambient FTOHs, but all are suitable for use in laboratory experiments.

3.2 PTR-ToF-MS: real-time detection of 4:2 FTOH degradation products

The experiments carried out in this work focused on the degradation of approximately 10 ppbv of 4:2 FTOH, in the absence of NO_x, at RHs of 22%, 44%, and 60%. Previous smog chamber studies have only investigated the reactivity of FTOHs, including the 4:2 FTOH, under dry conditions with $^{\bullet}OH$ radicals and chlorine (Cl) atoms, in both the presence and absence of NO_x.[18,80–84] The OH-initiated oxidation pathways of FTOHs were first proposed in 2004 (Fig. 1) and based on smog chamber experiments initiated with Cl atoms, as they react in the same manner with FTOHs as $^{\bullet}OH$ radicals.[18] In this initial study, the *in situ* FTIR analysis of FTOH oxidation products suggested the formation of PFCAs at yields below 10%. Due to the low yields and overlapping IR spectra of PFCAs, FTIR lacked the sensitivity and specificity needed for their definitive identification or quantification. Instead, an offline analysis using liquid chromatography tandem mass spectrometry revealed that each FTOH produced a corresponding PFCA retaining the full perfluorinated chain (*i.e.*, 8:2 FTOH produced perfluorononanoic acid). These analyses also showed the formation of a homologous series of shorter-chain PFCAs; for example, the oxidation of 8:2 FTOH resulted in PFCAs ranging from trifluoroacetic acid upward. Additionally, ^{19}F NMR detected perfluorinated acid fluorides, which can hydrolyze to their corresponding carboxylic acids, thereby providing further evidence for PFCA formation during FTOH atmospheric oxidation. As a result, various studies have since concluded that, in a low NO_x or NO_x-free environment, the atmospheric oxidation of FTOHs results in the aldehyde product in a yield close to 100%.[18,23,80,81,85] Thus, the expected first generation oxidation product here was the 4:2 fluorotelomer aldehyde (4:2 FTAL; $CF_3(CF_2)_3CH_2CHO$). Further oxidation of 4:2 FTAL has been reported to yield the secondary products 4:2 fluorotelomer carboxylic acid (4:2 FTCA; $CF_3(CF_2)_3CH_2COOH$), 4:2 perfluorinated aldehyde (4:2 PFAL; $CF_3(CF_2)_3CHO$), and the corresponding peracid ($CF_3(CF_2)_3CH_2C(O)OOH$).[18,81]

During these experiments, the PTR-ToF-MS detected two degradation products – the primary 4:2 FTAL (m/z 263.011842) and the secondary 4:2 FTCA (m/z 279.006757). No subsequent oxidation products, such as PFCAs (*e.g.*, TFA), were detected under the described experimental conditions. This likely results from limitations of the PTR-ToF-MS being hindered for compounds with strong surface interactions and unfavourable PAs. For example, TFA[69] has a reported PA of 711.7 kJ mol^{-1}, which is comparable to that of water[69] and 4:2 FTOH[68] but lower still than those of commonly measured VOCs.[70,71] Additionally, while a secondary product was observed here, further oxidation to PFCAs is expected based on previous chamber and modelling studies[18,23] but would almost certainly be present below the detection limits of the instrument and require an additional chemical ionization mass spectrometer.[86] Nevertheless, as this study focused on demonstrating the feasibility of real-time PFAS oxidation kinetics and early-stage product identification, Fig. 2 clearly illustrates that as 4:2 FTOH degrades (blue trace), the 4:2 FTAL primary product signal (pink trace) initially increases before it starts to decrease upon reaction to form 4:2 FTCA (purple trace). This trend is also seen at RHs of 44% and 60% (Fig. S5). The 4:2 FTAL primary product can react with OH and photolyze. Available light in the OFR is provided at shorter wavelengths than the most abundant actinic photons, which could affect the observed interconversion rates here. In comparing the cross-sections of the 1:2 and 6:2 FTALs at different wavelengths[85,87] (Table S7), it is possible for photolysis of 4:2 FTAL to occur at 254 nm. However, secondary photolytic product yields within the OFR here are likely underestimated as less photolysis is likely to occur at shorter wavelengths.[85,87] Without calibration standards for the 4:2 FTAL and 4:2 FTCA, we cannot calculate product yields for comparison to previous studies.[87] A third peak of interest was also noted (m/z 260.996192; Fig. S5), which we suspect to be the dehydrated form of the 4:2 FTCA. Based on previously reported PTR-MS product-ion fragmentation of non-fluorinated organic acids, the dehydrated 4:2 FTCA may have been formed *via* the loss of water following protonation *via* hydronium.[88] Similar ionization has been previously observed for acetic acid[89] and is believed to result here in an elemental formula of $CF_3(CF_2)_3CH_2C(O)^+$, with the positive charge on the carbonyl carbon.[88] As with our calibrations for the 4:2 FTOH, the PTR-MS sensitivity towards the detected products decreases with increasing RH.[88–90]

As shown by their widespread global distribution, including to remote regions, some PFAS can undergo long-range atmospheric transport (*i.e.*, neutral, volatile PFAS like FTOHs) or transport *via* global ocean currents (*i.e.*, ionic PFAS).[13,23] With the gas-phase oxidation of FTOHs to PFCAs expected to be more prevalent in remote locations where NO_x concentrations are low,[18,23] this NO_x-free work should be more atmospherically representative of such environments. Previous NO_x-free experiments primarily investigated FTOH reaction mechanisms with Cl atoms. This was done for two main reasons: (i) Cl atoms can be a reliable proxy for $^{\bullet}OH$ radicals and (ii) Cl atoms can be more cleanly generated than $^{\bullet}OH$ radicals in a Pyrex smog chamber. Where Cl atoms were produced *via* the photolysis of Cl_2, $^{\bullet}OH$ radicals were generated by photolyzing methyl nitrite – generating NO as a byproduct.[91] Other techniques have been used in recent years to cleanly generate $^{\bullet}OH$ radicals, such as hydrogen peroxide (H_2O_2) in an Ingeniven FEP Teflon Gas Sampling Bag to observe hydrofluoroether oxidation.[25] Historically, the photolysis of H_2O_2 in Pyrex smog chambers fitted with FTIR has been avoided due to the presence of water vapour. These limitations demonstrate the advantages of the described OFR approach here. Since the mechanism of OH oxidation with 4:2 FTOH under NO_x-free conditions was previously inferred from Cl-initiated experiments, our results ultimately show that

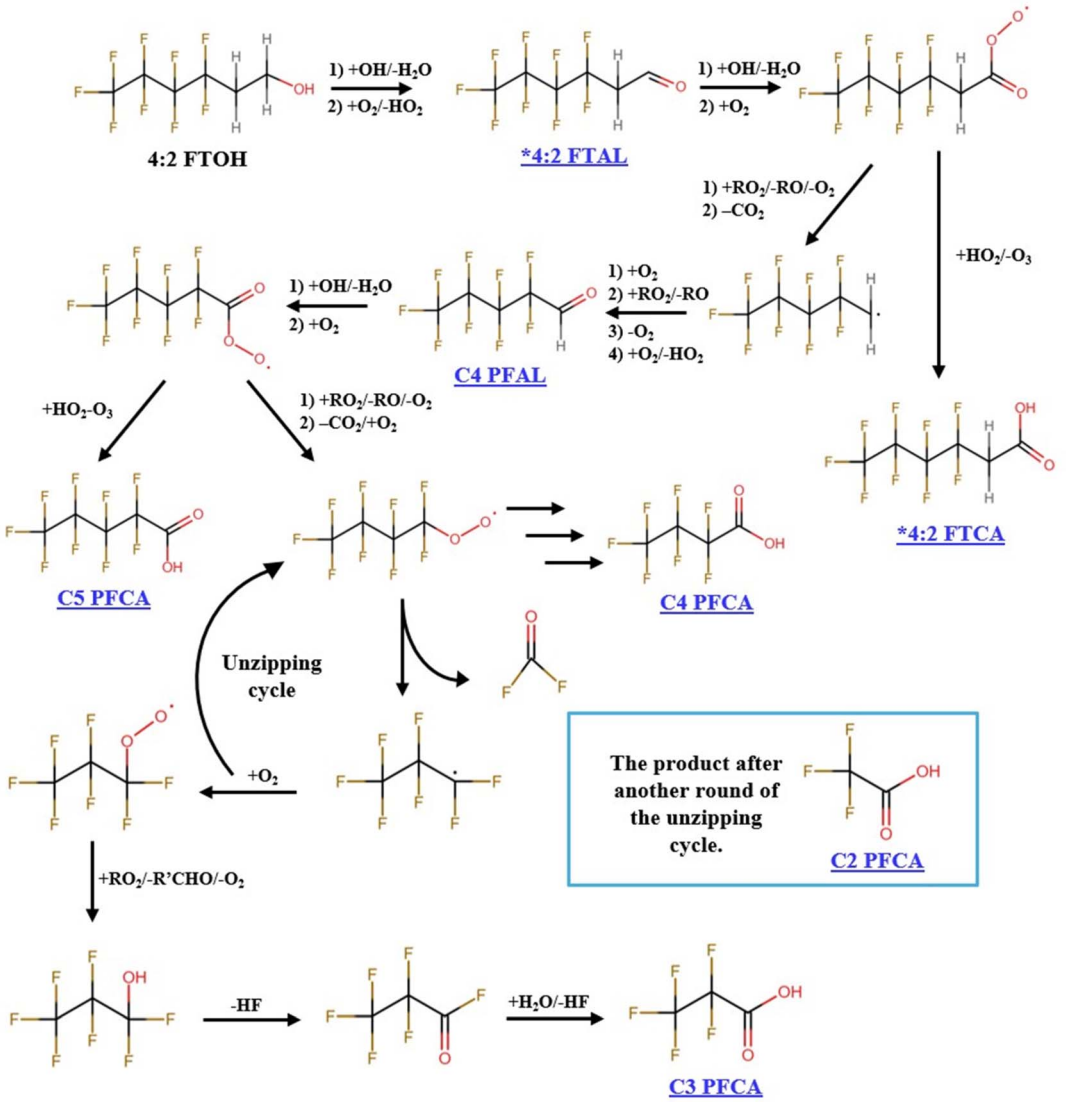

Fig. 1 The proposed atmospheric degradation mechanism of the 4:2 FTOH + ˙OH radicals in a NO_x-free environment.[18] The expected stable end products are underlined in blue, with the specific products observed in this work being asterisked. The compounds shown are as follows: 4:2 fluorotelomer aldehyde (4:2 FTAL); 4:2 fluorotelomer carboxylic acid (4:2 FTCA); perfluoropentanal (C_4 PFAL); perfluoropentanoic acid (C_5 PFCA); perfluorobutanoic acid (C_4 PFCA); pentafluoropropionic acid (C_3 PFCA); trifluoroacetic acid (C_2 PFCA).

the mechanism under OH-initiated, NO_x-free conditions is consistent with those predictions.

3.3 Oxidation kinetics: OH initiated reaction of 4:2 FTOH

The rate constant for the reactivity of ˙OH radicals with the 4:2 FTOH was determined by measuring the decrease in signal as a function of OH exposure. From the blank-corrected and normalized data, the observed rate constant, k_{obs} (cm^3 $molecule^{-1}$ s^{-1}), for the oxidation of 4:2 FTOH was determined using eqn (1).[41]

$$\ln \frac{[4:2\ \mathrm{FTOH}]}{[4:2\ \mathrm{FTOH}]_0} = \ln\left(\frac{I}{I_0}\right) = -k_{obs}[\mathrm{OH}]t \qquad (1)$$

Here $[4:2\ FTOH]_0$ is the initial 4:2 FTOH concentration (molecules cm^{-3}) and [4:2 FTOH] is the measured 4:2 FTOH concentration (molecules cm^{-3}) at a given OH exposure (molecules s cm^{-3}), which is the product of the OH concentration ([OH], molecules cm^{-3}) and the average residence time (t) in the OFR (s). The I_0 and I terms are the signal intensities (ncps) for the 4:2 FTOH in the absence and presence of ˙OH radicals, respectively. The reaction is a bimolecular process following a pseudo-first-order reaction, with 4:2 FTOH in excess relative to OH. The value of k_{obs} was determined by plotting the natural logarithm of the intensity ratios against OH exposure (Fig. 3). At the three different RHs explored here, the k_{obs} values (Fig. 3a and Table S3) were $(1.0 \pm 0.1) \times 10^{-12}$, $(6.5 \pm 0.4) \times 10^{-13}$, and $(6.3 \pm 0.1) \times 10^{-13}$ cm^3 $molecules^{-1}$ s^{-1} at 22%, 44%, and 60% RH, respectively. The linear regression coefficients indicate good linearity at all RHs, with $R^2 \geq 0.97$ (Table S3). Statistical analyses (t-test) were performed and the rate constant at 22% RH was significantly different from those at both 44% and 60% RH ($p < 1 \times 10^{-6}$), whereas no statistically

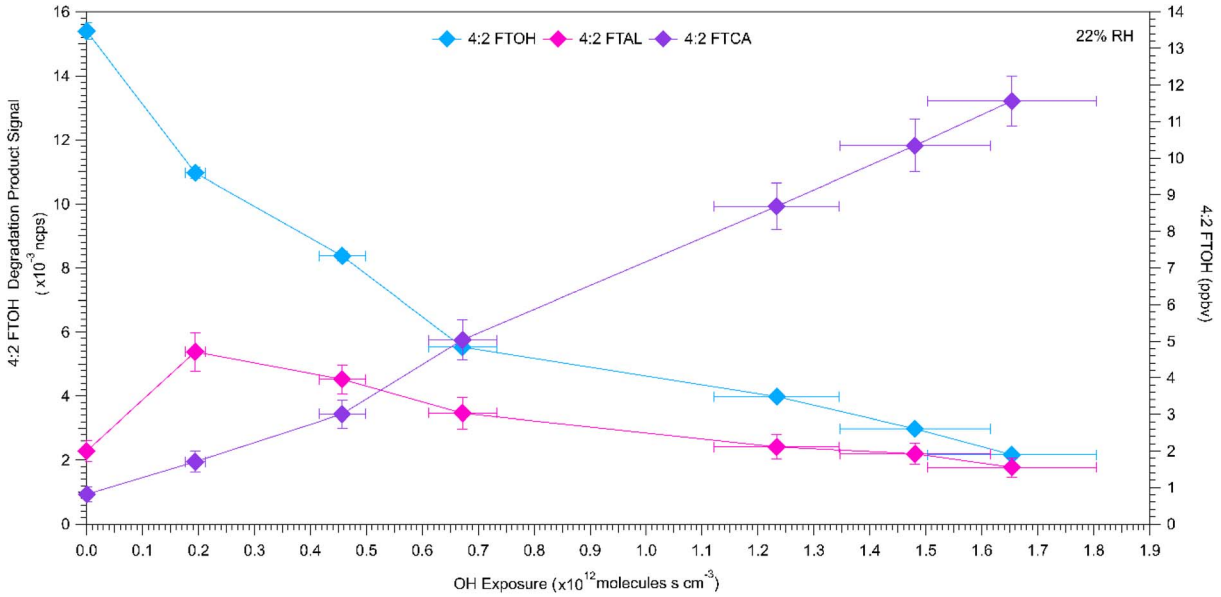

Fig. 2 The change in 4:2 FTOH (ppbv; *m*/*z* 265.027492) and the detected degradation products (4:2 FTAL, *m*/*z* 263.11842; 4:2 FTCA, *m*/*z* 279.006757; ncps) with increasing OH exposure (molecules s cm^{-3}) at 22% RH. The right *y*-axis depicts the decreasing mixing ratio of permeating 4:2 FTOH, and the propagated error at each point, as it reacts with $^{\bullet}$OH radicals. On the left *y*-axis are the normalized average signals of the degradation products, with each point's corresponding standard deviation. The *x*-axis shows the OH exposure and the propagated error at each point.

significant difference was observed between 44% and 60% RH ($p = 0.26$). This suggests that the reaction behaviour changes appreciably between 22% and 44% RH but remains relatively stable at higher humidity levels.

In the only study which reported the OH oxidation rate of 4:2 FTOH in the presence of NO_x and under dry conditions, the rate constant was $(1.07 \pm 0.22) \times 10^{-12}$ cm^3 $molecules^{-1}$ s^{-1}.[80] The k_{obs} values measured here are the same order of magnitude. The results are also consistent when compared to kinetic data for the 1:2 and 6:2 FTOHs (Table 1), where chain-length has been found to not affect the kinetics of longer-chained FTOH reactions with OH.[13] It should also be noted that the 4:2 FTOH rate constants measured at 44% and 60% RH are 37% slower (Table S3 and Section S3). Water may induce greater wall effects or altered PTR-MS sensitivity. The 4:2 FTOH could diffuse to the surface of the OFR (417 s) within the experimental residence time (468 s), leading to the potential for wall losses. The instrument response was also calculated at each RH by fitting to single and double exponential functions to account for any changes from surface effects in the OFR and of the PTR-MS sampling inlet. Previously, instrument and inlet surface effects for highly surface active gases (*e.g.*, hydrochloric acid) have been characterized by fitting decay curves to a double exponential.[92–95] Since the 4:2 FTOH is much more volatile and unable to ionize, it is not surprising that system response times were marginally affected resulting in k_{obs} that were higher by ~25% at the two higher RHs when taking these into account with the double exponential approach.

The final average OH reaction rate constant values at 44% and 60% RH are $(7.4 \pm 0.8) \times 10^{-13}$ and $(7.2 \pm 0.8) \times 10^{-13}$ cm^3 $molecules^{-1}$ s^{-1}, respectively, when averaging the results obtained from all three calculation approaches (Table 1). Statistical analyses (*t*-test) were performed and the 'original' k_{obs} at 22% RH was found to be significantly different from both averaged k_{obs} at 44% and 60% RH ($p < 1 \times 10^{-4}$). However, no statistically significant difference was observed between the averaged rate constants at 44% and 60% RH ($p = 0.79$). Although a statistically significant decrease in the observed rate constants was found between 22% and ≥44% RH, the described experimental setup does not allow us to distinguish between a water vapour dependence of the 4:2 FTOH oxidation and systematic effects associated with increased RH, including diffusion driven wall interactions. While diffusion timescale estimates and exponential fitting analyses suggest that such effects are unlikely to fully account for the observed difference, they cannot be completely ruled out. This suggests that the reaction behaviour differs notably between 22% and 44% RH and increasing it further to 60% RH does not result in statistically significant additional change. Thus, we cannot reliably say that the averaged 44% and 60% RH rate constants are different or that diffusion driven wall interactions are contributing to the slower rates.

Another advantage of using OFR-PTR-ToF-MS in this work is its ability to directly study the decay of 4:2 FTOH with $^{\bullet}$OH radicals. Previously reported chamber experiments have investigated the degradation and reactivity of FTOHs with $^{\bullet}$OH radicals[80,82,83] and Cl atoms[18,81–84] in both the presence and absence of NO_x; however, these experiments were done only under dry conditions. It should first be noted that saturated FTOHs, such as 4:2 FTOH and the structurally related 12 FTOH, do not react appreciably with O_3 under atmospheric conditions. Negative control experiments performed with O_3 did not detect any change in FTOH concentration at experimental timescales, consistent with previous findings that reported an atmospheric

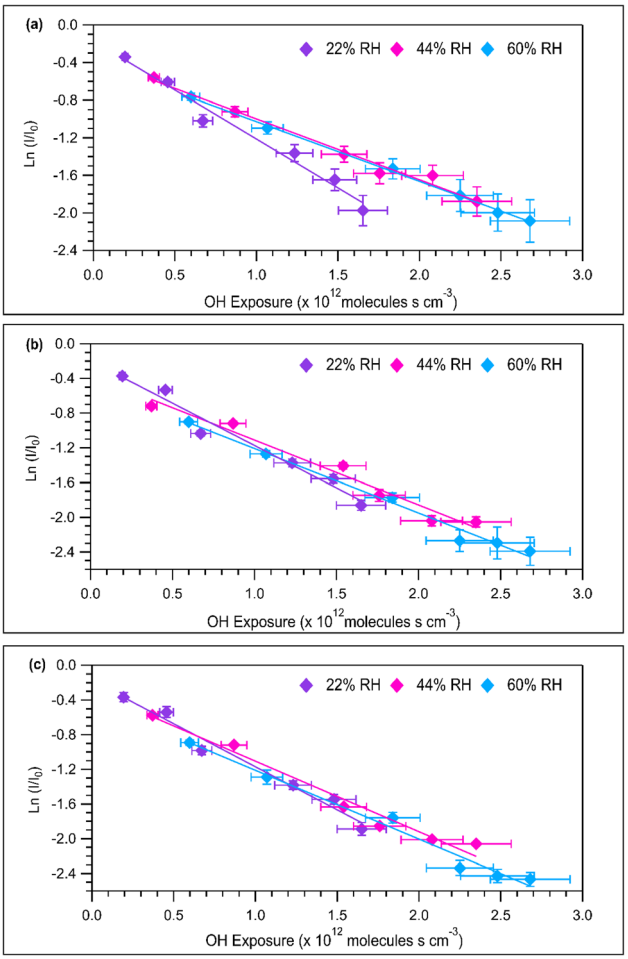

Fig. 3 Loss of the 4:2 FTOH following reaction with ˙OH radicals at different OH exposures and RHs. The response time of this method is shown here in the (a) original data as well as after being fitted to (b) single and (c) double exponential functions. The k_{obs} values were determined using a linear regression analysis weighted to the error in the y-axis. The k_{obs} values for the three different data sets can be found in Table S3.

lifetime of approximately 5900 days for 12 FTOH with respect to reaction with O_3, assuming a background concentration of 40 ppb.[82] Together, these observations demonstrate that O_3 is not responsible for any measurable loss of 4:2 FTOH in our experiments. Consequently, the decay of 4:2 FTOH in the OFR is dominated by reaction with ˙OH radicals. Ultimately, the atmospheric fate of FTOH is likely limited by reaction with OH,[13] as more than 90% of FTOHs oxidize *via* hydrogen abstraction at the carbon adjacent to the alcohol group.[80,84] Both radicals are electrophilic with modest steric demands and both reactions are exothermic; thus, the abstraction behaviour of Cl atoms and ˙OH radicals are expected to be similar.[96] While Cl atoms have shown to be a good surrogate for ˙OH radicals, they are not perfect proxies due to differing regional selectivity.[97] This experimental setup allows the study of OH chemistry in the presence of water vapour instead of requiring Cl atoms. Consequently, the work described here contains the first measured rate constants made for the reaction between 4:2 FTOH and ˙OH radicals at different RHs. The described OFR-PTR-ToF-MS technique is not limited by the presence of humidity, like FTIR, and can instead study chemistry under more atmospherically relevant conditions and make kinetic measurements on the timescale of seconds as opposed to minutes.[98] While previous research on PFCA precursors achieved good time resolution and observed similar degradation products, continuous high time resolution opens the door to study faster aspects of this gas-phase chemistry.[74,75,86,99,100] In an atmospheric context, humidity and light can vary on timescales of minutes to hours while the abundance of radicals can change on timescales of seconds. To observe such chemistry requires fast, *in situ* measurement techniques that capture rapidly shifting effects, which the PTR-MS is capable of.[86] In the context of chamber experiments, the high temporal resolution is beneficial to the observation of real-time reaction kinetics as well as the potential to detect transient intermediates. Ultimately, we suspect that while this greater time resolution may not be important for the study of all compounds, it could be beneficial for some and should be applied when possible.

4 Atmospheric implications/future directions

For the first time, 4:2 FTOH degradation kinetics and products were measured at varying RHs relevant to the range found in the atmosphere. The potential effects of RH on the gas-phase

Table 1 Summary of the 4:2 FTOH + OH rate constants found within this study at different RHs compared to the previously determined value under dry conditions, as well as those constants determined for the 1:2 and 6:2 FTOHs. The 4:2 FTOH k_{obs} at 22% RH is the 'original' rate constant while those at 44% and 60% RH are reported as an average of the three calculation approaches described in the main text

Analyte	Rate constant (cm^3 $molecules^{-1}$ s^{-1})	RH (%)	Method	Reference
4:2 FTOH.	$(1.0 \pm 0.1) \times 10^{-12}$	22	OFR coupled to PTR-ToF-MS	This work
$CF_3(CF_2)_3CH_2CH_2OH$	$(7.4 \pm 0.8) \times 10^{-13}$	44		
	$(7.2 \pm 0.8) \times 10^{-13}$	60		
	$(1.07 \pm 0.22) \times 10^{-12}$	0	Relative rate	Ellis *et al.*, 2003
1:2 FTOH, $CF_3CH_2CH_2OH$	$(8.9 \pm 0.3) \times 10^{-13}$		Pulsed laser photolysis-laser-induced fluorescence	Kelly *et al.*, 2005
	$(1.08 \pm 0.05) \times 10^{-12}$		Relative rate	
	$(6.91 \pm 0.91) \times 10^{-13}$			Hurley *et al.*, 2005
6:2 FTOH, $CF_3(CF_2)_5CH_2CH_2OH$	$(7.9 \pm 0.8) \times 10^{-13}$			Kelly *et al.*, 2005

kinetics of FTOHs, and PFAS in general, is not well understood within the literature and requires further investigation. Previous work has shown that RH can accelerate and decelerate the kinetics of non-fluorinated alcohols (20% to 95% RH).[33–38] Although the mechanism for a potential RH enhancement of 4:2 FTOH is not yet known, studies of similar molecules may provide insight into possible reaction pathways. Previous work on small alcohols (*e.g.*, ethanol and *n*-propanol) suggest that water can enhance reaction rates by forming weak complexes with both the alcohol and OH.[34] These complexes can increase the effective collision probability as well as stabilize the transition state, making product formation more favourable. Further evidence is needed for 4:2 FTOH, as this water-assisted effect is reaction-specific since the influence of water varies between systems,[35] before a plausible mechanism for the water vapour dependence in our experiments can be proposed.

The PTR-ToF-MS detected the 4:2 FTAL and the 4:2 FTCA. In the future, if calibrations can be conducted, the identified degradation products can be further investigated as a function of OH exposure or RH. Our observed rate coefficients at 22%, 44%, and 60% RH were similar in magnitude to the literature value reported at 0% RH,[80] although lower rates were observed at higher RH. The latter cannot be conclusively attributed to a role for water vapour in the kinetics as experimental errors inherent to the OFR and PTR-ToF-MS cannot be ruled out. The primary objective of this work was to evaluate the feasibility of combining an OFR with PTR-ToF-MS to measure PFAS oxidation kinetics and to provide initial constraints on OH reaction kinetics for 4:2 FTOH under varying RH conditions. As the RH issues experienced here do not negate the kinetic findings, the results presented in this work highlight the need for continued investigation into the role of water vapour in the atmospheric oxidation of volatile PFAS and provides a foundation for improving mechanistic understanding of these processes in future studies.

While our experimental technique allows real-time study of 4:2 FTOH oxidation under atmospherically relevant RH, several limitations should be noted. High RH can influence instrument sensitivity and may contribute to systematic biases reflected in measured rate constants. The radical chemistry within the OFR may also differ from atmospheric conditions due to elevated HO_2 concentrations, which can alter product distributions. Additionally, this approach is most effective for volatile or semi-volatile species with favourable PAs, making detection of stable end products such as short-chain PFCAs challenging. Complementary analytical techniques may be required to observe full degradation to terminal oxidation products. Despite these limitations, this approach provides valuable real-time constraints on early-stage PFAS oxidation chemistry by detecting intermediates and highlights directions for future improvements. Ultimately, this work demonstrates the power of the OFR-PTR-ToF-MS as a useful real-time measurement technique to study gas-phase transformations of volatile PFAS within a laboratory setting. With an ability to study atmospherically realistic oxidative chemistry at different RHs, the described instrumental setup has the potential to study suspected, but uncharacterized, mechanisms of atmospheric PFAS formation and degradation.

Author contributions

Alessia A. Colussi performed the chamber experiments and data analysis. Alessia A. Colussi wrote the manuscript with contributions from all authors. All authors were involved in examining and reviewing the results. All authors were involved in editing the manuscript.

Conflicts of interest

The authors declare that they do not have any conflicts of interest associated with this work.

Data availability

The data supporting this article has been included as part of the supplementary information (SI). Supplementary information is available. See DOI: https://doi.org/10.1039/d5em00943j.

Acknowledgements

We thank Amy Leithead, Dr Jeremy Wentzell, Dr Chao Peng, Lisa Azzarello, Dr Qifan Liu, and Dr Teles Furlani for experimental support. Alessia A. Colussi acknowledges funding from the Ontario Graduate Scholarship. Partial funding for this work was provided by the Chemicals Management Plan of the Government of Canada.

References

1 L. Ahrens, M. Shoeib, T. Harner, S. C. Lee, R. Guo and E. J. Reiner, Wastewater treatment plant and landfills as sources of polyfluoroalkyl compounds to the atmosphere, *Environ. Sci. Technol.*, 2011, **45**(19), 8098–8105.
2 Y. Tian, Y. Yao, S. Chang, Z. Zhao, Y. Zhao, X. Yuan, F. Wu and H. Sun, Occurrence and phase distribution of neutral and ionizable per-and polyfluoroalkyl substances (PFASs) in the atmosphere and plant leaves around landfills: a case study in Tianjin, China, *Environ. Sci. Technol.*, 2018, **52**(3), 1301–1310.
3 I. T. Cousins, J. C. DeWitt, J. Glüge, G. Goldenman, D. Herzke, R. Lohmann, C. A. Ng, M. Scheringer and Z. Wang, The high persistence of PFAS is sufficient for their management as a chemical class, *Environ. Sci.: Processes Impacts*, 2020, **22**(12), 2307–2312.
4 F. Pérez, M. Nadal, A. Navarro-Ortega, F. Fàbrega, J. L. Domingo, D. Barceló and M. Farré, Accumulation of perfluoroalkyl substances in human tissues, *Environ. Int.*, 2013, **59**, 354–362.
5 V. M. Vieira, K. Hoffman, H. M. Shin, J. M. Weinberg, T. F. Webster and T. Fletcher, Perfluorooctanoic acid exposure and cancer outcomes in a contaminated community: a geographic analysis, *Environ. Health Perspect.*, 2013, **121**(3), 318–323.

6 P. Sun, X. Nie, X. Chen, L. Yin, J. Luo, L. Sun, C. Wan and S. Jiang, Nrf2 signaling elicits a neuroprotective role against PFOS-mediated oxidative damage and apoptosis, *Neurochem. Res.*, 2018, **43**(12), 2446–2459.
7 S. E. Fenton, A. Ducatman, A. Boobis, J. C. DeWitt, C. Lau, C. Ng, J. S. Smith and S. M. Roberts, Per-and polyfluoroalkyl substance toxicity and human health review: Current state of knowledge and strategies for informing future research, *Environ. Toxicol. Chem.*, 2021, **40**(3), 606–630.
8 J. P. Giesy and K. Kannan, Global distribution of perfluorooctane sulfonate in wildlife, *Environ. Sci. Technol.*, 2001, **35**(7), 1339–1342.
9 G. T. Tomy, W. Budakowski, T. Halldorson, P. A. Helm, G. A. Stern, K. Friesen, K. Pepper, S. A. Tittlemier and A. T. Fisk, Fluorinated organic compounds in an eastern Arctic marine food web, *Environ. Sci. Technol.*, 2004, **38**(24), 6475–6481.
10 S. Valdersnes, B. M. Nilsen, J. F. Breivik, A. Borge and A. Maage, Geographical trends of PFAS in cod livers along the Norwegian coast, *PLoS One*, 2017, **12**(5), e0177947.
11 D. Muir, R. Bossi, P. Carlsson, M. Evans, A. De Silva, C. Halsall, C. Rauert, D. Herzke, H. Hung, R. Letcher and F. Rigét, Levels and trends of poly-and perfluoroalkyl substances in the Arctic environment–An update, *Emerging Contam.*, 2019, **5**, 240–271.
12 A. M. Roos, M. Gamberg, D. Muir, A. Kärrman, P. Carlsson, C. Cuyler, Y. Lind, R. Bossi and F. Rigét, Perfluoroalkyl substances in circum-Arctic Rangifer: caribou and reindeer, *Environ. Sci. Pollut. Res.*, 2022, **29**(16), 23721–23735.
13 C. J. Young and S. A. Mabury, Atmospheric perfluorinated acid precursors: chemistry, occurrence, and impacts, *Reviews of environmental contamination and toxicology*. 2010, 208, pp. 1–09.
14 A. M. P. Sulbaek, O. J. Nielsen, M. D. Hurley, J. C. Ball, T. J. Wallington, D. A. Ellis, J. W. Martin and S. A. Mabury, Atmospheric chemistry of 4: 2 fluorotelomer alcohol (n-C4F9CH2CH2OH): products and mechanism of Cl atom initiated oxidation in the presence of NO x, *J. Phys. Chem. A*, 2005, **109**(9), 1849–1856.
15 H. J. Lehmler, Synthesis of environmentally relevant fluorinated surfactants—a review, *Chemosphere*, 2005, **58**(11), 1471–1496.
16 J. W. Martin, D. C. Muir, C. A. Moody, D. A. Ellis, W. C. Kwan, K. R. Solomon and S. A. Mabury, Collection of airborne fluorinated organics and analysis by gas chromatography/chemical ionization mass spectrometry, *Anal. Chem.*, 2002, **74**(3), 584–590.
17 Dupont Global PF, Strategy Update: Presentation to USEPAOPPT, January 31, 2005, US Public Docket AR, 1914, **226**.
18 D. A. Ellis, J. W. Martin, A. O. De Silva, S. A. Mabury, M. D. Hurley, M. P. Sulbaek Andersen and T. J. Wallington, Degradation of fluorotelomer alcohols: a likely atmospheric source of perfluorinated carboxylic acids, *Environ. Sci. Technol.*, 2004, **38**(12), 3316–3321.
19 H. Nilsson, A. Kärrman, A. Rotander, B. van Bavel, G. Lindström and H. Westberg, Inhalation exposure to fluorotelomer alcohols yield perfluorocarboxylates in human blood?, *Environ. Sci. Technol.*, 2010, **44**(19), 7717–7722.
20 N. L. Stock, F. K. Lau, D. A. Ellis, J. W. Martin, D. C. Muir and S. A. Mabury, Polyfluorinated telomer alcohols and sulfonamides in the North American troposphere, *Environ. Sci. Technol.*, 2004, **38**(4), 991–996.
21 A. Jahnke, L. Ahrens, R. Ebinghaus and C. Temme, Urban versus remote air concentrations of fluorotelomer alcohols and other polyfluorinated alkyl substances in Germany, *Environ. Sci. Technol.*, 2007, **41**(3), 745–752.
22 J. Li, S. Del Vento, J. Schuster, G. Zhang, P. Chakraborty, Y. Kobara and K. C. Jones, Perfluorinated compounds in the Asian atmosphere, *Environ. Sci. Technol.*, 2011, **45**(17), 7241–7248.
23 T. J. Wallington, M. D. Hurley, J. D. Xia, D. J. Wuebbles, S. Sillman, A. Ito, J. E. Penner, D. A. Ellis, J. Martin, S. A. Mabury and O. J. Nielsen, Formation of C7F15COOH (PFOA) and other perfluorocarboxylic acids during the atmospheric oxidation of 8: 2 fluorotelomer alcohol, *Environ. Sci. Technol.*, 2006, **40**(3), 924–930.
24 H. M. Pickard, A. S. Criscitiello, C. Spencer, M. J. Sharp, D. C. Muir, A. O. De Silva and C. J. Young, Continuous non-marine inputs of per-and polyfluoroalkyl substances to the High Arctic: a multi-decadal temporal record, *Atmos. Chem. Phys.*, 2018, **18**(7), 5045–5058.
25 A. P. Folkerson, S. R. Schneider, J. P. Abbatt and S. A. Mabury, Avoiding regrettable replacements: can the introduction of novel functional groups move PFAS from recalcitrant to reactive?, *Environ. Sci. Technol.*, 2023, **57**(44), 17032–17041.
26 J. T. Gerig, *Fluorine Nmr. Biophysics Textbook Online*, 2001, pp. 1–35.
27 X. Zhang, A. He, R. Guo, Y. Zhao, L. Yang, S. Morita, Y. Xu, I. Noda and Y. Ozaki, A new approach to removing interference of moisture from FTIR spectrum, *Spectrochim. Acta Mol. Biomol. Spectrosc.*, 2022, **265**, 120373.
28 L. G. Huey, D. R. Hanson and C. J. Howard, Reactions of SF6-and I-with atmospheric trace gases, *J. Phys. Chem.*, 1995, **99**(14), 5001–5008.
29 D. L. Slusher, L. G. Huey, D. J. Tanner, F. M. Flocke and J. M. Roberts, A thermal dissociation–chemical ionization mass spectrometry (TD-CIMS) technique for the simultaneous measurement of peroxyacyl nitrates and dinitrogen pentoxide, *J. Geophys. Res. Atmos.*, 2004, **109**, D19315.
30 B. H. Lee, F. D. Lopez-Hilfiker, C. Mohr, T. Kurtén, D. R. Worsnop and J. A. Thornton, An iodide-adduct high-resolution time-of-flight chemical-ionization mass spectrometer: Application to atmospheric inorganic and organic compounds, *Environ. Sci. Technol.*, 2014, **48**(11), 6309–6317.
31 P. Brophy and D. K. Farmer, A switchable reagent ion high resolution time-of-flight chemical ionization mass spectrometer for real-time measurement of gas phase

oxidized species: characterization from the 2013 southern oxidant and aerosol study., *Atmos. Meas. Tech.*, 2015, **8**(7), 2945–2959.

32 F. D. Lopez-Hilfiker, S. Iyer, C. Mohr, B. H. Lee, E. L. D'Ambro, T. Kurtén and J. A. Thornton, Constraining the sensitivity of iodide adduct chemical ionization mass spectrometry to multifunctional organic molecules using the collision limit and thermodynamic stability of iodide ion adducts, *Atmos. Meas. Tech.*, 2016, **9**(4), 1505–1512.

33 R. A. Jara-Toro, F. J. Hernández, R. A. Taccone, S. I. Lane and G. A. Pino, Water Catalysis of the Reaction between Methanol and OH at 294 K and the Atmospheric Implications, *Angew. Chem., Int. Ed.*, 2017, **56**(8), 2166–2170.

34 R. A. Jara-Toro, F. J. Hernández, M. D. Garavagno, R. A. Taccone and G. A. Pino, Water catalysis of the reaction between hydroxyl radicals and linear saturated alcohols (ethanol and n-propanol) at 294 K, *Phys. Chem. Chem. Phys.*, 2018, **20**(44), 27885–27896.

35 W. Chao, J. Jr-Min Lin, K. Takahashi, A. Tomas, L. Yu, Y. Kajii, S. Batut, C. Schoemaecker and C. Fittschen, Water vapor does not catalyze the reaction between methanol and OH radicals, *Angew. Chem., Int. Ed.*, 2019, **58**(15), 5013–5017.

36 L. Xu, N. T. Tsona, S. Tang, J. Li and L. Du, Role of (H2O) n (n= 1–2) in the gas-phase reaction of ethanol with hydroxyl radical: mechanism, kinetics, and products, *ACS Omega*, 2019, **4**(3), 5805–5817.

37 I. Weber, H. Bouzidi, B. Krumm, C. Schoemaecker, A. Tomas and C. Fittschen, Water does not catalyze the reaction of OH radicals with ethanol, *Phys. Chem. Chem. Phys.*, 2020, **22**(14), 7165–7168.

38 E. M. Neeman, D. González, S. Blázquez, B. Ballesteros, A. Canosa, M. Antiñolo, L. Vereecken, J. Albaladejo and E. Jiménez, The impact of water vapor on the OH reactivity toward CH3CHO at ultra-low temperatures (21.7–135.0 K): Experiments and theory, *J. Chem. Phys.*, 2021, **155**(3), 034306.

39 K. Li, J. Liggio, C. Han, Q. Liu, S. G. Moussa, P. Lee and S. M. Li, Understanding the impact of high-NO x conditions on the formation of secondary organic aerosol in the photooxidation of oil sand-related precursors, *Environ. Sci. Technol.*, 2019, **53**(24), 14420–14429.

40 K. Li, J. Liggio, P. Lee, C. Han, Q. Liu and S. M. Li, Secondary organic aerosol formation from α-pinene, alkanes, and oil-sands-related precursors in a new oxidation flow reactor, *Atmos. Chem. Phys.*, 2019, **19**(15), 9715–9731.

41 Q. Liu, J. Liggio, K. Li, P. Lee and S. M. Li, Understanding the impact of relative humidity and coexisting soluble iron on the OH-initiated heterogeneous oxidation of organophosphate flame retardants, *Environ. Sci. Technol.*, 2019, **53**(12), 6794–6803.

42 W. J. Massman, Molecular diffusivities of Hg vapor in air, O2 and N2 near STP and the kinematic viscosity and thermal diffusivity of air near STP, *Atmos. Environ.*, 1999, **33**(3), 453–457.

43 Z. Peng and J. L. Jimenez, Radical chemistry in oxidation flow reactors for atmospheric chemistry research, *Chem. Soc. Rev.*, 2020, **49**(9), 2570–2616.

44 B. B. Palm, P. Campuzano-Jost, A. M. Ortega, D. A. Day, L. Kaser, W. Jud, T. Karl, A. Hansel, J. F. Hunter, E. S. Cross and J. H. Kroll, In situ secondary organic aerosol formation from ambient pine forest air using an oxidation flow reactor, *Atmos. Chem. Phys.*, 2016, **16**(5), 2943–2970.

45 W. H. Brune, The chamber wall index for gas–Wall interactions in atmospheric environmental enclosures, *Environ. Sci. Technol.*, 2019, **53**(7), 3645–3652.

46 A. T. Lambe, T. B. Onasch, D. R. Croasdale, J. P. Wright, A. T. Martin, J. P. Franklin, P. Massoli, J. H. Kroll, M. R. Canagaratna, W. H. Brune and D. R. Worsnop, Transitions from functionalization to fragmentation reactions of laboratory secondary organic aerosol (SOA) generated from the OH oxidation of alkane precursors, *Environ. Sci. Technol.*, 2012, **46**(10), 5430–5437.

47 J. L. Jimenez, M. R. Canagaratna, N. M. Donahue, A. S. Prevot, Q. Zhang, J. H. Kroll, P. F. DeCarlo, J. D. Allan, H. Coe, N. L. Ng and A. C. Aiken, Evolution of organic aerosols in the atmosphere, *science*, 2009, **326**(5959), 1525–1529.

48 D. S. Tkacik, A. T. Lambe, S. Jathar, X. Li, A. A. Presto, Y. Zhao, D. Blake, S. Meinardi, J. T. Jayne, P. L. Croteau and A. L. Robinson, Secondary organic aerosol formation from in-use motor vehicle emissions using a potential aerosol mass reactor, *Environ. Sci. Technol.*, 2014, **48**(19), 11235–11242.

49 Z. Peng and J. L. Jimenez, Modeling of the chemistry in oxidation flow reactors with high initial NO, *Atmos. Chem. Phys.*, 2017, **17**(19), 11991–12010.

50 X. Ma, K. Li, S. Zhang, Z. Yang, L. Xu, N. Tsona Tchinda and L. Du, Oxidation Flow Reactor and Its Application in Secondary Organic Aerosol Formation in Laboratory Studies, *ACS ES&T Air*, 2025, **2**(8), 1394–1410.

51 I. J. George, A. Vlasenko, J. G. Slowik, K. Broekhuizen and J. P. Abbatt, Heterogeneous oxidation of saturated organic aerosols by hydroxyl radicals: uptake kinetics, condensed-phase products, and particle size change, *Atmos. Chem. Phys.*, 2007, **7**(16), 4187–4201.

52 Z. Peng, D. A. Day, H. Stark, R. Li, J. Lee-Taylor, B. B. Palm, W. H. Brune and J. L. Jimenez, HO x radical chemistry in oxidation flow reactors with low-pressure mercury lamps systematically examined by modeling, *Atmos. Meas. Tech.*, 2015, **8**(11), 4863–4890.

53 J. P. Rowe, A. T. Lambe and W. H. Brune, Effect of varying the λ= 185 and 254 nm photon flux ratio on radical generation in oxidation flow reactors, *Atmos. Chem. Phys. Discuss.*, 2020, **7**, 1–5.

54 H. Czech, P. Yli-Pirilä, P. Tiitta, M. Ihalainen, A. Hartikainen, E. Schneider, P. Martens, A. Paul, T. Hohaus, C. P. Rüger and J. Jokiniemi, The effect of aging conditions at equal OH exposure in an oxidation flow reactor on the composition of toluene-derived

secondary organic aerosols, *Environ. Sci.: Atmos.*, 2024, **4**(7), 718–731.

55 Q. Liu, J. Liggio, D. Wu, A. Saini, S. Halappanavar, J. J. Wentzell, T. Harner, K. Li, P. Lee and S. M. Li, Experimental study of OH-initiated heterogeneous oxidation of organophosphate flame retardants: Kinetics, mechanism, and toxicity, *Environ. Sci. Technol.*, 2019, **53**(24), 14398–14408.

56 Y. Liu and S. P. Sander, Rate Constant for the OH + CO Reaction at Low Temperatures, *J. Phys. Chem. A*, 2015, **119**(39), 10060–10066, DOI: 10.1021/acs.jpca.5b07220.

57 J. Mao, X. Ren, W. H. Brune, J. R. Olson, J. H. Crawford, A. Fried, L. G. Huey, R. C. Cohen, B. Heikes, H. B. Singh and D. R. Blake, Airborne measurement of OH reactivity during INTEX-B, *Atmos. Chem. Phys.*, 2009, **9**(1), 163–173.

58 R. S. Blake, P. S. Monks and A. M. Ellis, Proton-transfer reaction mass spectrometry, *Chem. Rev.*, 2009, **109**(3), 861–896.

59 J. De Gouw and C. Warneke, Measurements of volatile organic compounds in the earth's atmosphere using proton-transfer-reaction mass spectrometry, *Mass Spectrom. Rev.*, 2007, **26**(2), 223–257.

60 A. Jordan, S. G. Haidacher, G. Hanel, E. Hartungen, L. Märk, H. Seehauser, R. Schottkowsky, P. Sulzer and T. D. Märk, A high resolution and high sensitivity proton-transfer-reaction time-of-flight mass spectrometer (PTR-TOF-MS), *Int. J. Mass Spectrom.*, 2009, **286**(2–3), 122–128.

61 S. M. Li, A. Leithead, S. G. Moussa, J. Liggio, M. D. Moran, D. Wang, K. Hayden, A. Darlington, M. Gordon, R. Staebler and P. A. Makar, Differences between measured and reported volatile organic compound emissions from oil sands facilities in Alberta, Canada, *Proc. Natl. Acad. Sci. U. S. A.*, 2017, **114**(19), E3756–E3765.

62 S. N. Wren, J. Liggio, Y. Han, K. Hayden, G. Lu, C. M. Mihele, R. L. Mittermeier, C. Stroud, J. J. Wentzell and J. R. Brook, Elucidating real-world vehicle emission factors from mobile measurements over a large metropolitan region: a focus on isocyanic acid, hydrogen cyanide, and black carbon, *Atmos. Chem. Phys.*, 2018, **18**(23), 16979–17001.

63 M. Lao, L. R. Crilley, L. Salehpoor, T. C. Furlani, I. Bourgeois, J. A. Neuman, A. W. Rollins, P. R. Veres, R. A. Washenfelder, C. C. Womack and C. J. Young, A portable, robust, stable and tunable calibration source for gas-phase nitrous acid (HONO), *Atmos. Meas. Tech. Discuss.*, 2020, **2020**, 1–31.

64 T. C. Furlani, R. Ye, J. Stewart, L. R. Crilley, P. M. Edwards, T. F. Kahan and C. J. Young, Development and validation of a new in situ technique to measure total gaseous chlorine in air, *Atmos. Meas. Tech.*, 2023, **16**(1), 181–193.

65 M. J. Tang, M. Shiraiwa, U. Pöschl, R. A. Cox and M. Kalberer, Compilation and evaluation of gas phase diffusion coefficients of reactive trace gases in the atmosphere: Volume 2. Diffusivities of organic compounds, pressure-normalised mean free paths, and average Knudsen numbers for gas uptake calculations, *Atmos. Chem. Phys.*, 2015, **15**, 5585–5598.

66 A. K. Lee, J. P. Abbatt, W. R. Leaitch, S. M. Li, S. J. Sjostedt, J. J. Wentzell, J. Liggio and A. M. Macdonald, Substantial secondary organic aerosol formation in a coniferous forest: observations of both day-and nighttime chemistry, *Atmos. Chem. Phys.*, 2016, **16**(11), 6721–6733.

67 C. Wu, C. Wang, S. Wang, W. Wang, B. Yuan, J. Qi, B. Wang, H. Wang, C. Wang, W. Song and X. Wang, Measurement report: Important contributions of oxygenated compounds to emissions and chemistry of volatile organic compounds in urban air, *Atmos. Chem. Phys.*, 2020, **20**(23), 14769–14785.

68 T. Delatour, L. Menin, B. Eriksen, N. Gasilova, C. Mujahid and X. Theurillat, Dielectric barrier discharge ionization procures characteristic adducts of polyfluoroalkyl substances (PFAS) amenable by gas chromatography-mass spectrometry, *Microchem. J.*, 2024, **204**, 111012.

69 E. P. Hunter and S. G. Lias, Evaluated gas phase basicities and proton affinities of molecules: an update, *J. Phys. Chem. Ref. Data*, 1998, **27**(3), 413–656.

70 J. Long and B. Munson, Proton affinities of some oxygenated compounds, *J. Am. Chem. Soc.*, 1973, **95**(8), 2427–2432.

71 G. Bouchoux, D. A. Buisson, S. Bourcier and M. Sablier, Application of the kinetic method to bifunctional bases: ESI tandem quadrupole experiments, *Int. J. Mass Spectrom.*, 2003, **228**(2–3), 1035–1054.

72 A. K. Lee, J. P. Abbatt, W. R. Leaitch, S. M. Li, S. J. Sjostedt, J. J. Wentzell, J. Liggio and A. M. Macdonald, Substantial secondary organic aerosol formation in a coniferous forest: observations of both day-and nighttime chemistry, *Atmos. Chem. Phys.*, 2016, **16**(11), 6721–6733.

73 J. Krechmer, F. Lopez-Hilfiker, A. Koss, M. Hutterli, C. Stoermer, B. Deming, J. Kimmel, C. Warneke, R. Holzinger, J. Jayne and D. Worsnop, Evaluation of a new reagent-ion source and focusing ion–molecule reactor for use in proton-transfer-reaction mass spectrometry, *Anal. Chem.*, 2018, **90**(20), 12011–12018.

74 A. R. Jensen, A. R. Koss, R. B. Hales and J. A. de Gouw, Measurements of volatile organic compounds in ambient air by gas-chromatography and real-time Vocus PTR-TOF-MS: calibrations, instrument background corrections, and introducing a PTR Data Toolkit, *Atmos. Meas. Tech.*, 2023, **16**(21), 5261–5285.

75 T. P. Riedel, J. R. Lang, M. J. Strynar, A. B. Lindstrom and J. H. Offenberg, Gas-phase detection of fluorotelomer alcohols and other oxygenated per-and polyfluoroalkyl substances by chemical ionization mass spectrometry, *Environ. Sci. Technol. Lett.*, 2019, **6**(5), 289–293.

76 J. M. Mattila and J. H. Offenberg, Measuring Short-Chain per- and Polyfluoroalkyl Substances in Central New Jersey Air Using Chemical Ionization Mass Spectrometry, *J. Air Waste Manage. Assoc.*, 2024, **74**(8), 531–539, DOI: 10.1080/10962247.2024.2366491.

77 M. Shoeib, T. Harner and P. Vlahos, Perfluorinated chemicals in the Arctic atmosphere, *Environ. Sci. Technol.*, 2006, **40**(24), 7577–7583.

78 J. L. Barber, U. Berger, C. Chaemfa, S. Huber, A. Jahnke, C. Temme and K. C. Jones, Analysis of per-and polyfluorinated alkyl substances in air samples from Northwest Europe, *J. Environ. Monit.*, 2007, **9**(6), 530–541.

79 A. M. Lin, J. T. Thompson, J. P. Koelmel, Y. Liu, J. A. Bowden and T. G. Townsend, Landfill gas: a major pathway for neutral per-and polyfluoroalkyl substance (PFAS) release, *Environ. Sci. Technol. Lett.*, 2024, **11**(7), 730–737.

80 D. A. Ellis, J. W. Martin, S. A. Mabury, M. D. Hurley, M. P. Sulbaek Andersen and T. J. Wallington, Atmospheric lifetime of fluorotelomer alcohols, *Environ. Sci. Technol.*, 2003, **37**(17), 3816–3820.

81 M. D. Hurley, J. C. Ball, T. J. Wallington, M. P. Sulbaek Andersen, D. A. Ellis, J. W. Martin and S. A. Mabury, Atmospheric chemistry of 4: 2 fluorotelomer alcohol (CF3 (CF2) 3CH2CH2OH): Products and mechanism of Cl atom initiated oxidation, *J. Phys. Chem. A*, 2004, **108**(26), 5635–5642.

82 M. D. Hurley, J. A. Misner, J. C. Ball, T. J. Wallington, D. A. Ellis, J. W. Martin, S. A. Mabury and M. P. Sulbaek Andersen, Atmospheric Chemistry of CF3CH2CH2OH: Kinetics, Mechanisms and Products of Cl Atom and OH Radical Initiated Oxidation in the Presence and Absence of NO X, *J. Phys. Chem. A*, 2005, **109**(43), 9816–9826.

83 T. Kelly, V. Bossoutrot, I. Magneron, K. Wirtz, J. Treacy, A. Mellouki, H. Sidebottom and G. Le Bras, A kinetic and mechanistic study of the reactions of OH radicals and Cl atoms with 3, 3, 3-trifluoropropanol under atmospheric conditions, *J. Phys. Chem. A*, 2005, **109**(2), 347–355.

84 V. C. Papadimitriou, D. K. Papanastasiou, V. G. Stefanopoulos, A. M. Zaras, Y. G. Lazarou and P. Papagiannakopoulos, Kinetic study of the reactions of Cl atoms with $CF_3CH_2CH_2OH$, $CF_3CF_2CH_2OH$, $CHF_2CF_2CH_2OH$, and $CF_3CHFCF_2CH_2OH$, *J. Phys. Chem. A*, 2007, **111**(45), 11608–11617.

85 M. S. Chiappero, F. E. Malanca, G. A. Argüello, S. T. Wooldridge, M. D. Hurley, J. C. Ball, T. J. Wallington, R. L. Waterland and R. C. Buck, Atmospheric chemistry of perfluoroaldehydes (C x F2 x+ 1CHO) and fluorotelomer aldehydes (C x F_2 x+ $1CH_2CHO$): quantification of the important role of photolysis, *J. Phys. Chem. A*, 2006, **110**(43), 11944–11953.

86 C. J. Young, S. Joudan, Y. Tao, J. J. Wentzell and J. Liggio, High time resolution ambient observations of gas-phase perfluoroalkyl carboxylic acids: implications for atmospheric sources, *Environ. Sci. Technol. Lett.*, 2024, **11**(12), 1348–1354.

87 S. R. Sellevåg, T. Kelly, H. Sidebottom and C. J. Nielsen, A study of the IR and UV-Vis absorption cross-sections, photolysis and OH-initiated oxidation of CF 3 CHO and CF 3 CH 2 CHO, *Phys. Chem. Chem. Phys.*, 2004, **6**(6), 1243–1252.

88 D. Pagonis, K. Sekimoto and J. De Gouw, A library of proton-transfer reactions of H3O+ ions used for trace gas detection, *J. Am. Soc. Mass Spectrom.*, 2019, **30**(7), 1330–1335.

89 M. Baasandorj, D. B. Millet, L. Hu, D. Mitroo and B. J. Williams, Measuring acetic and formic acid by proton-transfer-reaction mass spectrometry: sensitivity, humidity dependence, and quantifying interferences, *Atmos. Meas. Tech.*, 2015, **8**(3), 1303–1321.

90 L. Ernle, N. Wang, G. Bekö, G. Morrison, P. Wargocki, C. J. Weschler and J. Williams, Assessment of aldehyde contributions to PTR-MS m/z 69.07 in indoor air measurements, *Atmos. Meas. Tech. Discuss.*, 2023, **3**(9), 1286–1295.

91 C. M. Butt, C. J. Young, S. A. Mabury, M. D. Hurley and T. J. Wallington, Atmospheric Chemistry of 4: 2 Fluorotelomer Acrylate [C4F9CH2CH2OC (O) CH□ CH2]: Kinetics, Mechanisms, and Products of Chlorine-Atom- and OH-Radical-Initiated Oxidation, *J. Phys. Chem. A*, 2009, **113**(13), 3155–3161.

92 M. S. Zahniser, D. D. Nelson, B. McManus, P. L. Kebabian and D. Lloyd, Measurement of trace gas fluxes using tunable diode laser spectroscopy, *Philos. Trans. R. Soc. London, A*, 1995, **351**(1696), 371–382.

93 R. A. Ellis, J. G. Murphy, E. Pattey, R. Van Haarlem, J. M. O'Brien and S. C. Herndon, Characterizing a quantum cascade tunable infrared laser differential absorption spectrometer (QC-TILDAS) for measurements of atmospheric ammonia, *Atmos. Meas. Tech.*, 2010, **3**(2), 397–406.

94 A. Moravek, S. Singh, E. Pattey, L. Pelletier and J. G. Murphy, Measurements and quality control of ammonia eddy covariance fluxes: a new strategy for high-frequency attenuation correction, *Atmos. Meas. Tech.*, 2019, **12**(11), 6059–6078.

95 T. C. Furlani, P. R. Veres, K. E. Dawe, J. A. Neuman, S. S. Brown, T. C. VandenBoer and C. J. Young, Validation of a new cavity ring-down spectrometer for measuring tropospheric gaseous hydrogen chloride, *Atmos. Meas. Tech. Discuss.*, 2021, 1–30.

96 M. L. Poutsma, Evolution of structure–reactivity correlations for the hydrogen abstraction reaction by chlorine atom, *J. Phys. Chem. A*, 2013, **117**(4), 687–703.

97 M. L. Poutsma, Evolution of structure–reactivity correlations for the hydrogen abstraction reaction by hydroxyl radical and comparison with that by chlorine atom, *J. Phys. Chem. A*, 2013, **117**(30), 6433–6449.

98 C. J. Young, M. D. Hurley, T. J. Wallington and S. A. Mabury, Atmospheric chemistry of 4: 2 fluorotelomer iodide (n-C4F9CH2CH2I): Kinetics and products of photolysis and reaction with OH radicals and Cl atoms, *J. Phys. Chem. A*, 2008, **112**(51), 13542–13548.

99 P. Veres, J. M. Roberts, C. Warneke, D. Welsh-Bon, M. Zahniser, S. Herndon, R. Fall and J. de Gouw, Development of negative-ion proton-transfer chemical-ionization mass spectrometry (NI-PT-CIMS) for the measurement of gas-phase organic acids in the atmosphere, *Int. J. Mass Spectrom.*, 2008, **274**(1–3), 48–55.

100 B. B. Bowers, J. A. Thornton and R. C. Sullivan, Evaluation of iodide chemical ionization mass spectrometry for gas and aerosol-phase per-and polyfluoroalkyl substances (PFAS) analysis, *Environ. Sci.: Processes Impacts*, 2023, **25**(2), 277–287.